Minimization of environment-induced decoherence in quantum subsystems and application to solid-state-based quantum gates

M. Wenin* and W. Pötz†

Institut für Physik, Theory Division Karl Franzens Universität Graz, Universitätsplatz 5, 8010 Graz, Austria

(Received 19 May 2008; revised manuscript received 22 August 2008; published 21 October 2008)

A general formulation of optimal control theory for open quantum systems (quantum subsystems) based on a superoperator method is presented. This approach is applied to a computation of optimized time-dependent fields for solid-state-based realizations of quantum gates. Decoherence is incorporated within the spin-boson model and treated within, essentially, the Bloch-Redfield formalism. Generating a "decoherence-free subspace" for the superoperator dynamically, we identify optimal trajectories in the phase space of the dynamical system for one- and two-qubit subsystems. Numerical analysis shows that, for the ideal case where one has full control over the subsystem's Hamiltonian, any gate operation can be realized with arbitrary small loss of coherence due to dephasing and optimal solutions exist which are independent of both spectral density and the temperature of the environment. At the example of a Josephson charge quantum gate we study the more realistic situation where one has a restricted number of control fields which, while providing a universal gate, cannot completely eliminate dephasing.

DOI: 10.1103/PhysRevB.78.165118 PACS number(s): 32.80.Qk, 73.63.Kv, 03.67.Pp, 03.65.Yz

I. INTRODUCTION

An essential prerequisite for quantum computation is precise coherent control of quantum two-level systems, so-called qubits. Several proposals for solid-state-based quantum gate realizations, such as quantum dots or superconducting quantum interference devices (SQUIDs), have been made and qubits, as well as coupled qubits (quantum gates), have been investigated both theoretically and experimentally.[1–19] Any realization of a quantum gate, however, is a quantum subsystem. Coherent manipulation of the quantum gate is disturbed by unwanted interaction with its environment, ultimately leading to decoherence and dissipation. It is thus an important task to find ways to minimize or even eliminate this interaction in order to maintain coherent quantum dynamics for as long as it is necessary to perform the calculation. Apart from design optimization there is an approach of minimizing decoherence in quantum subsystems by selecting optimal pulse shapes for the external control within experimental capabilities. To find such time-dependent control fields theoretically, one may resort to optimal control theory.[20] Target state preparation of a quantum system evolving out of a specific initial state, for example the system's ground state, has been well investigated with applications throughout quantum physics.[21–27]

The situation becomes demanding when one considers a quantum subsystem. Quantum computation, moreover, requires state-independent control when a quantum gate operation is to be executed.[28–32] Important progress has been made in the study of unitary operations in isolated systems.[33–36] The temporal evolution of such systems is fully characterized by the unitary time-evolution operator. For dissipative quantum systems, the superoperator approach provides a natural formalism to describe state-independent transformations.[37] In this paper we therefore formulate the optimality condition for steering a quantum subsystem in terms of the time-evolution superoperator.

This paper is organized as follows. In Sec. II we formulate the general superoperator approach. The optimal control problem in terms of the time-evolution superoperator and the cost functional are formulated in Sec. III. In Sec. IV the spin-boson model is incorporated into this superoperator formulation within second-order perturbation theory in the spin-boson interaction (Bloch-Redfield approach). In Sec. V we map single and double Josephson charge qubits onto the spin-boson model and study them numerically. Dynamical generation of decoherence-free subspaces for one- and two-qubit systems is explored. Numerical examples for coupled qubits are given both for idealized and realistic control situations. Conclusions and relevance of this work for experiment are given. Section VI gives a summary of the main aspects of the paper. Technical details regarding perturbation theory for the superoperator and the definition of the decoherence function are summarized in Appendixes A and B. Throughout the paper we use the Einstein summation convention.

II. GENERAL APPROACH

The kinetic equation for the density matrix of a subsystem $\rho(t)$ interacting with an environment is of the general form

$$i\hbar\dot{\rho} = [H(t),\rho] + D[t,\rho], \quad \rho(0) = \rho_0. \tag{1}$$

The time-dependent Hamiltonian $H(t)$ of the subsystem contains the external control fields $\varepsilon_j(t)$ and the dissipator $D[t,\rho]$ accounts for the interaction between system and environment.[38] In general the dissipator is time-dependent and may depend on the control fields $\varepsilon_j(t)$. Within the superoperator formalism, Eq. (1) takes the form

$$i\hbar\dot{\rho}(t) = [\mathcal{L}(t) + \mathcal{D}(t)]\rho(t). \tag{2}$$

Here $\mathcal{L}(t)\rho(t) \equiv [H(t),\rho(t)]$ is the Liouville superoperator and $\mathcal{D}(t)\rho(t) \equiv D[t,\rho]$ is the dissipation superoperator. To obtain a state-independent formulation we introduce the time-evolution superoperator $\mathcal{X}(t)$ defined through

$$\rho(t) = \mathcal{X}(t)\rho(0). \tag{3}$$

With this ansatz we enter Eq. (2) to obtain the equation of motion for $\mathcal{X}(t)$,

$$i\hbar\dot{\mathcal{X}}(t) = [\mathcal{L}(t) + \mathcal{D}(t)]\mathcal{X}(t), \quad \mathcal{X}(0) = \mathbb{1}_L. \tag{4}$$

$\mathbb{1}_L$ is the unit operator in the superoperator space. The formal solution is provided by

$$\mathcal{X}(t) = T_{\leftarrow} \exp\left\{-\frac{i}{\hbar}\int_0^t [\mathcal{L}(t') + \mathcal{D}(t')]dt'\right\}, \tag{5}$$

where $T_{\leftarrow}$ denotes the chronological time-ordering operator which orders products of time-dependent (super) operators such that their time arguments increase from right to left. In the absence of dissipation the superoperator $\mathcal{X}(t)$ is determined by the unitary time-evolution operator of the system $U(t)=T_{\leftarrow}\exp\{-\frac{i}{\hbar}\int_0^t H(t')dt'\}$, viz.

$$\mathcal{X}_{ijrs}(t) = U_{ir}(t)U^{\dagger}_{sj}(t). \tag{6}$$

III. SUPEROPERATOR FORMULATION OF THE OPTIMIZATION PROBLEM

Let $\mathcal{O}$ be the desired target operation, specified up to a global phase, which is to be executed during the time interval $[0,t_f]$ and completed at target time t_f. The target state for any valid initial state $\rho(0)$ of the subsystem is thus

$$\rho(t_f) = \mathcal{O}\rho(0)\mathcal{O}^{\dagger}. \tag{7}$$

The target superoperator $\mathcal{X}_T$ has the form

$$\mathcal{X}_T|_{ijrs} \equiv \mathcal{O}_{ir}\mathcal{O}^{\dagger}_{sj}.$$

For a purely coherent dynamics (isolated quantum system) one obtains the condition for $U(t_f)$

$$\mathcal{X}_{ijrs}(t_f) = U_{ir}(t_f)U^{\dagger}_{sj}(t_f) = \mathcal{X}_T|_{ijrs}. \tag{8}$$

Per definition, complete control over the isolated quantum system implies that this inverse problem can be solved and at least one set of control fields that meets this condition exists. For a quantum subsystem, the dissipator in Eq. (4) in general does not allow to reach the target superoperator $\mathcal{X}_T$ exactly. Based on Eq. (8), however, we define a cost functional with the goal to arrive at the target superoperator $\mathcal{X}_T$ as accurately as possible,

$$\mathcal{J} = \|\mathcal{X}(t_f) - \mathcal{X}_T\|^2 \equiv \sum_{p,q,m,j} |\mathcal{X}_{pqmj}(t_f) - \mathcal{O}_{pm}\mathcal{O}^{\dagger}_{jq}|^2 \to \min. \tag{9}$$

To minimize $\mathcal{J}$, a variation in the external control contained in $H(t)$ needs to be performed. The optimization of the cost functional (9) is a standard inverse problem in optimal control theory.[20]

Without dissipation and using the expression Eq. (6) we obtain[28] for Eq. (9)

$$\mathcal{J}_u = N - \frac{1}{N}|\mathrm{Tr}\{U(t_f)\mathcal{O}^{+}\}|^2. \tag{10}$$

Here N is the dimension of the Hilbert space. We note that Eq. (9), as well as Eq. (10), is insensitive to a potential phase difference between $\mathcal{O}$ and $U(t_f)$.

In earlier work[26,39] on weakly dissipative quantum systems we have used, in addition to terms similar to Eq. (10), the contribution

$$\mathcal{J}_D = \langle \mathrm{Tr}\{[\rho^I(t_f) - \rho(0)]^2\}\rangle \tag{11}$$

to account for dissipation during quantum gate operation within first-order perturbation theory, leading to a cost functional $\mathcal{J}_{uD}=\mathcal{J}_u+\mathcal{J}_D$. $\mathcal{J}_D$ measures, in the interaction picture, the deviation of the initial state from the final state. In the absence of the dissipator, all initial states remain constant in time $\rho^I(t_f)=\rho(0)$. One can show that Eq. (9) contains Eqs. (10) and (11).

IV. SUPEROPERATOR FORMALISM FOR THE SPIN-BOSON MODEL: BLOCH-REDFIELD DISSIPATOR AND KINETIC EQUATIONS

The spin-boson model is a widely used and thoroughly investigated system to describe dissipation and decoherence in open quantum systems.[38,40–42] It has been used frequently to model solid-state realizations of elementary quantum systems for quantum computation purposes.[17,42] We therefore adopt this model and subject it to the superoperator optimization formalism outlined above, whereby the dissipator is computed within second order in the spin-boson interaction.

A. Hamiltonian of the system

To describe a qubit system, we use the computational basis (orthonormal states) $\{|1\rangle,|2\rangle\}$ for one qubit and the product states $|1\rangle|1\rangle\equiv|1\rangle$, $|1\rangle|2\rangle\equiv|2\rangle$, $|2\rangle|1\rangle\equiv|3\rangle$, and $|2\rangle|2\rangle\equiv|4\rangle$ for two qubits. The total Hamiltonian is given by

$$H_T = H(t) + \sum_{\alpha=1}^{W} H_B^{\alpha} + H_I. \tag{12}$$

Here $H(t)$ is the time-dependent control Hamiltonian of the system and H_B^{α} are the Hamiltonians of the reservoirs. In the notation of second quantization, H_B^{α} takes the form

$$H_B^{\alpha} = \sum_{\mathbf{q}} \hbar\omega_{\mathbf{q}}^{\alpha}(b_{\mathbf{q}}^{\alpha})^{\dagger}b_{\mathbf{q}}^{\alpha}. \tag{13}$$

$(b_{\mathbf{q}}^{\alpha})^{\dagger}$ and $b_{\mathbf{q}}^{\alpha}$ are creation and annihilation operators of the bath α and the oscillator mode $\mathbf{q}$ with frequency $\omega_{\mathbf{q}}^{\alpha}$, respectively. W in Eq. (12) takes the values 1 for a single bath and 2 for two uncorrelated baths. The interaction Hamiltonian H_I for one single qubit is of the form

$$H_I = \sigma_z \otimes \sum_{\mathbf{q}} g_{\mathbf{q}}(b_{\mathbf{q}}^{\dagger} + b_{\mathbf{q}}). \tag{14}$$

$g_{\mathbf{q}}$ is the coupling constant of mode $\mathbf{q}$. For the two-qubit case we have

$$H_I = (A_1 + A_2) \otimes \sum_{\mathbf{q}} g_{\mathbf{q}}(b_{\mathbf{q}}^\dagger + b_{\mathbf{q}}), \tag{15}$$

when both qubits are coupled to the same bath and

$$H_I = \sum_{\alpha=1}^{2} A_\alpha \otimes \sum_{\mathbf{q}} g_{\mathbf{q}}^\alpha [(b_{\mathbf{q}}^\alpha)^\dagger + b_{\mathbf{q}}^\alpha], \tag{16}$$

when the qubits are coupled to two distinct reservoirs. We use $A_1 = \sigma_z \otimes \mathbb{1}$ and $A_2 = \mathbb{1} \otimes \sigma_z$ for system operators. $g_{\mathbf{q}}^\alpha$ are the relevant coupling constants. Thus we model an environment which causes pure dephasing in the computational basis. In fact, dephasing has been identified as the primary problem for Josephson-junction-based qubit realizations.[18]

B. Dissipation within the Bloch-Redfield superoperator

The Bloch-Redfield relaxation tensor (dissipation superoperator) is given by[41]

$$\mathcal{R}_{ijkl}(t) = \delta_{lj} \sum_r \Gamma_{irrk}^+(t) + \delta_{ik} \sum_r \Gamma_{lrrj}^-(t) - \Gamma_{ljik}^+(t) - \Gamma_{ljik}^-(t), \tag{17}$$

where the rates for two baths ($W=2$) are[43]

$$\Gamma_{ljik}^+(t) = \frac{1}{\hbar^2} U_{ip}(t) U_{kq}^*(t) \int_0^t dt' [C_1(t-t') P_{ljmn}^{(1)} + C_2(t-t') P_{ljmn}^{(2)}] U_{nq}(t') U_{mp}^*(t'), \tag{18}$$

$$\Gamma_{ljik}^-(t) = \frac{1}{\hbar^2} U_{lp}(t) U_{jq}^*(t) \int_0^t dt' [C_1(t'-t) P_{mnik}^{(1)} + C_2(t'-t) P_{mnik}^{(2)}] U_{nq}(t') U_{mp}^*(t'). \tag{19}$$

Here $U_{ip}(t)$ are the components of the unitary time-evolution operator, obtained by integration of Eq. (29) below, and $C_\alpha(t)$ are the system-bath-correlation functions.[42] Tracing out bath α yields

$$C_\alpha(t) = \mathrm{Tr}_{B_\alpha}\{B_\alpha(t) B_\alpha(0) \rho_\alpha^B\}. \tag{20}$$

with $B_\alpha = \Sigma_{\mathbf{q}} g_{\mathbf{q}}^\alpha [(b_{\mathbf{q}}^\alpha)^\dagger + b_{\mathbf{q}}^\alpha]$ and ρ_α^B as the canonical density operator of bath α.

The system-reservoir coupling enters in the operators $P^{(\alpha)}$. For a single qubit coupled to one bath we have $P_{ljmn}^{(1)} = (\sigma_z)_{lj}(\sigma_z)_{mn}$ and $P^{(2)}=0$. Using the matrices A_1 and A_2, we obtain for two distinct baths, $P_{ljmn}^{(\alpha)} = (A_\alpha)_{lj}(A_\alpha)_{mn}$, whereas for one common bath $P_{ljmn}^{(1)} = (A_1+A_2)_{lj}(A_1+A_2)_{mn}$ and $P_{ljmn}^{(2)}=0$.

We emphasize that we treat the time integrals in the expressions for the rates (18) and (19) exactly, avoiding the adiabatic approximation. This makes the problem computationally more demanding but is essential for obtaining control over dissipation and our results below. Moreover, we do not need the assumption of short memory times of the reservoirs.[38] Up to second order in the spin-boson interaction this approach is equivalent to a full non-Markovian treatment of the system.[44]

C. Expansion of the correlation functions into Laguerre polynomials

We expand the correlation functions using normalized Laguerre polynomials[45] $\varphi_K(x) = e^{-x/2} L_K(x)/K!$. In this way we can treat the integrals over time in Eqs. (18) and (19) in an efficient way since it allows us to parallelize the system of equations. If we choose an Ohmic spectral density $J_\alpha(\omega) = \eta_\alpha \omega e^{-\omega/\omega_c^\alpha}$ for all baths, we find for the correlator of Eq. (20)

$$C_\alpha(t-t') = \frac{\eta_\alpha (\omega_c^\alpha)^2}{[i - \omega_c^\alpha (t-t')]^2} + \frac{2\eta_\alpha}{\hbar^2 \beta_\alpha^2} \mathrm{Re}\left[\psi'\left(\frac{1 + i\omega_c^\alpha (t-t')}{\beta_\alpha \hbar \omega_c^\alpha}\right)\right]. \tag{21}$$

Here $\beta_\alpha \equiv 1/kT_\alpha$ is the inverse temperature of bath α and $\psi'(z)$ is the derivative of the digamma function. We note that

$$C_\alpha(t-t') = C_\alpha^*(t'-t). \tag{22}$$

For simplicity we choose for both baths identical parameter sets consisting of cutoff frequency ω_c, inverse temperature β, and coupling strength η. A more general approach is readily possible but at the expense of cumbersome notation. We define a dimensionless time $\tau = \omega_c t$. Omitting the index α, we have for $\tau - \tau' \geq 0$ (see Ref. 46),

$$C(\tau - \tau') \approx e^{-(\tau-\tau')/2} \sum_{K=0}^{N_{\max}} \sum_{J=0}^{K} \sum_{L=0}^{J} a_{KJL} \tau^L \tau'^{J-L}. \tag{23}$$

Here $N_{\max}$ is the number of Laguerre polynomials used to approximate the correlator. $a_{KJL} \equiv c_K d_{KJL}$ are expansion coefficients with

$$d_{KJL} = (-1)^L \frac{K!}{J!\,L!\,(K-J)!\,(J-L)!} \tag{24}$$

and

$$c_K = \int_0^\infty d\tau \varphi_K(\tau) C(\tau). \tag{25}$$

Equation (23) is not valid for $\tau - \tau' < 0$. To evaluate Eq. (19) we thus use Eq. (22) to obtain the correlator for negative time arguments.

D. Rates

Insertion of Eq. (23) into Eqs. (18) and (19) gives an explicit expression for the rates. It is convenient to define the following time-dependent auxiliary functions:

$$\mathcal{G}_{nqmp}^M(t) := (\omega_c t)^{-M} e^{-\omega_c t/2} \int_0^t dt' e^{\omega_c t'/2} (\omega_c t')^M U_{nq}(t') U_{mp}^*(t'), \tag{26}$$

where the index $M = J - L$ runs from 0 to $N_{\max}$. Using these functions we obtain for the rates

$$\Gamma^{+}_{ljik}(t) = \frac{1}{\hbar^2} U_{ip}(t) U^{*}_{kq}(t) [P^{(1)}_{ljmn} + P^{(2)}_{ljmn}] \times \sum_{K=0}^{N_{\max}} \sum_{J=0}^{K} \sum_{L=0}^{J} c_K d_{KJL} (\omega_c t)^J \mathcal{G}^{J-L}_{nqmp}(t), \quad (27)$$

and

$$\Gamma^{-}_{ljik}(t) = \frac{1}{\hbar^2} U_{lp}(t) U^{*}_{jq}(t) [P^{(1)}_{mnik} + P^{(2)}_{mnik}] \times \sum_{K=0}^{N_{\max}} \sum_{J=0}^{K} \sum_{L=0}^{J} c^{*}_K d_{KJL} (\omega_c t)^J \mathcal{G}^{J-L}_{nqmp}(t). \quad (28)$$

We use the right-hand sides of Eqs. (27) and (28) to compute the dissipator Eq. (17).

E. Closed set of kinetic equations

A system of coupled first-order ordinary differential equations describes the time evolution of the superoperator. It consists of the Schrödinger equation for the unitary time-evolution operator

$$i\hbar \dot{U}(t) = H(t) U(t), \quad U(0) = \mathbb{1}. \quad (29)$$

As follows from Eq. (26), the auxiliary functions are determined from

$$\dot{\mathcal{G}}^{M}_{nqmp}(t) = -\left(\frac{M}{t} + \frac{\omega_c}{2}\right) \mathcal{G}^{M}_{nqmp}(t) + U_{nq}(t) U^{*}_{mp}(t),$$

$$\mathcal{G}^{M}_{nqmp}(0) = 0. \quad (30)$$

The uppercase index $M=0,1,2\ldots$ in principle runs up to infinity, but for our examples convergence practically is reached for $M \approx 8$. The components $\mathcal{G}^{M}_{nqmp}(t)$, together with the components of $U(t)$, determine the Bloch-Redfield relaxation tensor $\mathcal{R}_{ijmn}(t)$. Finally, there is an equation of motion for the components of the time-evolution superoperator,

$$\dot{\mathcal{X}}_{ijrs}(t) = \left[-\frac{i}{\hbar} \mathcal{L}_{ijmn}(t) - \mathcal{R}_{ijmn}(t) \right] \mathcal{X}_{mnrs}(t),$$

$$\mathcal{X}_{ijrs}(0) = \delta_{ir} \delta_{js}. \quad (31)$$

Here the components of the system's Liouville superoperator are $\mathcal{L}_{ijmn}(t) = H_{im}(t) \delta_{nj} - H_{nj}(t) \delta_{im}$. Equations (29)–(31) present a closed set of differential equations which may now be solved efficiently in parallel.

V. NUMERICAL RESULTS

Having in mind solid-state realizations we map the Hamiltonian for a quantum gate realized by Josephson charge qubits onto the spin-boson model. Similar mappings have been performed for realizations of quantum gates via quantum dots.[42] The ideal single Josephson charge qubit is usually written in the eigenbasis of the Cooper-pair number operator using two charge states $\{|1\rangle, |2\rangle\}$ and is modeled by the Hamiltonian[13]

$$H_o(n_g, \Phi) = \sum_{n=1}^{2} 4E_C (n - n_g)^2 |n\rangle\langle n| - \frac{1}{2} E_J (|2\rangle\langle 1| + |1\rangle\langle 2|), \quad (32)$$

where E_C denotes the single-electron charging energy of the superconducting island and $E_J = E_J(\phi)$ is the Josephson coupling energy, which is a function of an externally applied magnetic flux ϕ; $n_g = \frac{C_g V_g}{2e}$ with C_g and V_g, respectively, denoting the gate capacitance and voltage. If the bias V_g is such that the qubit's working point is adjusted to a charge degeneracy point ($n_g \to n_g + \frac{1}{2}$), the effective Hamiltonian in matrix representation becomes

$$H_o(n_g, \Phi) = -\frac{1}{2} E_J(\phi) \sigma_x + 4E_C n_g \sigma_z.$$

In the absence of dissipation, the two control fields $\varepsilon_x(t) = -\frac{1}{2} E_J[\phi(t)]$ and $\varepsilon_z(t) = 4E_C n_g(t)$ allow the execution of arbitrary unitary single-qubit operations. Maintaining (near) unitary operations in the presence of state leakage and, in particular, dissipation is difficult.[47–49] Josephson charge qubits can be combined to a quantum gate with a Heisenberg-type qubit-qubit interaction as will be detailed below. In the absence of dissipation, it has been shown that there exist solutions for the four control fields such that, in principle, arbitrary quantum gate operations can be realized with arbitrary accuracy.[36]

We have in mind SQUIDs; however, we try to keep the discussion as general as possible to maintain relevance for other physical realizations of quantum gates which can be mapped on a spin-boson model for dephasing. As preparation for dealing with quantum gates, we first study the role of the fields ε_x and ε_z when controlling the single qubit individually and show, within the superoperator formalism, how one can generate decoherence-free superoperator subspaces dynamically. For the remainder of this section we discuss control of a quantum gate in presence of dephasing, first for an idealized control situation and then within experimental means.

A. Single-qubit control

We now discuss the one-qubit case for a system-reservoir interaction proportional to σ_z and investigate the control-bath interaction effects for two important cases, namely, when the control couples via σ_z (same direction as the bath) and when it couples via σ_x (perpendicular to the system-bath coupling). To be able to discuss the effects within analytical expressions, we choose a time-independent control.

1. Control coupling to σ_z

In the first example we consider a system with Hamiltonian

$$H_z = \frac{\hbar \omega_0}{2} \sigma_z. \quad (33)$$

We select the level-splitting frequency $\omega_0 = 2\varepsilon_z/\hbar$ as the only control corresponding to gate voltage control for SQUIDs to tune the island's charging energy. The time-evolution opera-

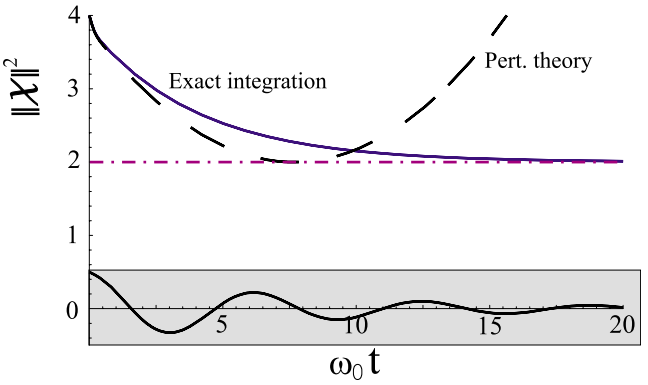

FIG. 1. (Color online) Time evolution of the norm $\|\mathcal{X}\|^2$, where the control is given by Eq. (33). The blue (dark gray) solid line corresponds to the exact (numerical) integration. Perturbation theory (black dashed line) gives $\|\chi\|^2=2+\kappa(t)^2$. The cyan (light gray) dotted-dashed line gives the asymptotic value of the superoperator norm. The lower part of the figure shows $\mathrm{Re}[\rho_{12}(t)]$ for the typical time evolution of a state. Parameters used for this calculation are $\omega_c=20\omega_0$, $\beta\hbar\omega_c=20$, and $\eta=0.01$.

tor $U(t)$ and the Bloch-Redfield dissipator are available analytically. The time-evolution superoperator is obtained within perturbation theory as explained in Appendix A. Evaluating the general expression (A5), we obtain for the nonvanishing elements

$$\mathcal{X}^{(1)}_{1111}(t)=\mathcal{X}^{(1)}_{2222}(t)=1, \tag{34}$$

$$\mathcal{X}^{(1)}_{1212}(t)=[\mathcal{X}^{(1)}_{2121}(t)]^*=e^{-i\omega_0 t}\kappa(t). \tag{35}$$

Here we define

$$\kappa(t)\equiv 1+2\eta\left\{\ln[1+(\omega_c t)^2]-4\psi^0\left(\frac{1}{\beta\hbar\omega_c}\right)\right\}+8\eta\,\mathrm{Re}\left[\psi^0\left(\frac{1+i\omega_c t}{\beta\hbar\omega_c}\right)\right], \tag{36}$$

and $\psi^0(z)\equiv\ln\Gamma(z)$. The real function $\kappa(t)$ reflects the role of the environment. It is equal to 1 for isolated systems. Using the projectors $P_\pm\equiv(1/2)(\mathbb{1}\pm\sigma_z)$ one can write the superoperator components in the limit $t\to\infty$ as

$$\mathcal{X}_{ijrs}(t\to\infty)=(P_+)_{ir}(P_+)_{sj}+(P_-)_{ir}(P_-)_{sj}. \tag{37}$$

In an exact treatment, the elements of Eq. (35) tend to zero. Thus for $t\to\infty$ every initial state ρ_0 loses its off-diagonal elements under the action of $\mathcal{X}$ (pure decoherence[38]). A numerical example is shown in Fig. 1 for illustration.

2. Control coupling to σ_x

We consider now a tunable coupling between the two basis states as facilitated by an external magnetic fields for SQUIDs. The system-control coupling is now proportional to σ_x and the system's Hamiltonian reads

$$H_x=\hbar\omega_0\sigma_x. \tag{38}$$

Inspection of the Bloch-Redfield dissipator shows that it is possible to decrease dissipation by applying high ω_0 values

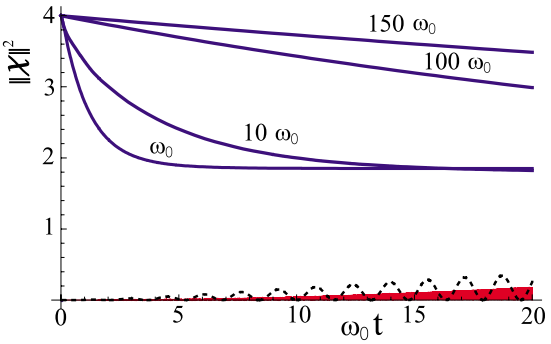

FIG. 2. (Color online) Time evolution of the norm $\|\mathcal{X}\|^2$, where the control here is given by Eq. (38). In this case interference effects allow a decrease in decoherence by increasing ω_0. The lower part of the figure shows the time evolution of $\mathrm{Tr}\{[\rho_u(t)-\rho(t)]^2\}$, where $\rho_u(t)$ corresponds to the unitary time evolution, for $\omega_0=1$ (black dotted line) and $\omega_0=150$ [red (dark gray) solid line], and $\rho(0)=(1,0;0,0)$. Parameters as in Fig. 1.

(dynamic decoupling) as demonstrated numerically in Fig. 2. In fact the Bloch-Redfield dissipator contains terms such as[10]

$$\int_0^t dt'\,C(t')\exp(2i\omega_0 t'), \tag{39}$$

where $C(t')$ is the correlation function (21), which vanishes for $\omega_0/\omega_c\to\infty$. The asymptotic value of the superoperator is now

$$\mathcal{X}_{ijrs}(t\to\infty)=\rho^{eq}_{ij}\delta_{rs}, \tag{40}$$

where ρ^{eq} is the thermal equilibrium state.[42] The superoperator projects any initial state ρ_0 into the same final state ρ^{eq}. The important lesson from a comparison of these two simple cases is that the nature of dissipation can be influenced by external control provided that the control fields couple with sufficient strength and can be applied on a time scale comparable or faster than that characteristic for the bath, i.e., $1/\omega_c$ in our case.

B. Control of quantum gates

1. "Decoherence free subspace" for the superoperator

The lesson learned for single qubits in the presence of dephasing are now put to use for the control of quantum gates. The Hamiltonian of Eq. (38) is associated with the unitary operator $U_{\mathrm{DF}}(t)=\exp(-itH_x/\hbar)$ and allows the reduction in the influence of the dissipator to arbitrary small values by increasing the frequency ω_0. Consider, for example, two qubits coupled to either two distinct baths or to one common bath always with a coupling proportional to σ_z. In both cases the Hamiltonian

$$H_{\mathrm{DF}}=\hbar\omega_0(\sigma_x\otimes\mathbb{1}+\mathbb{1}\otimes\sigma_x) \tag{41}$$

dynamically generates a time-evolution operator $U_{\mathrm{DF}}(t)$ which, for large values of $\omega_0\to\infty$, leads to decoherence-free overall time evolution. As usual, the decoherence-free subspace is defined as the set of all quantum states ρ^{DF}, for which $D[t,\rho^{\mathrm{DF}}]=0$ in Eq. (1) or, equivalently,

$$\mathcal{R}_{ijkl}(t)\rho_{kl}^{\mathrm{DF}}(t)=0 \quad \forall\, i,j. \tag{42}$$

It is constructed by dynamical decoupling of the open quantum system.[50–52] Following Eq. (6), we obtain a time-dependent superoperator $\mathcal{X}_{klrs}^{\mathrm{DF}}(t)=[U_{\mathrm{DF}}(t)]_{kr}[U_{\mathrm{DF}}^{\dagger}(t)]_{sr}$ that governs the time-evolution of an arbitrary state protected from environment-induced dissipation

$$\mathcal{R}_{ijkl}(t)\mathcal{X}_{klrs}^{\mathrm{DF}}(t)\to 0 \quad \forall\, i,j,r,s, \tag{43}$$

which may be viewed as the condition for defining the decoherence-free superoperator subspace.

This observation suggests the following control strategy. If the system is fully controllable (single-qubit operations plus arbitrary qubit-qubit interaction) each target operator $\mathcal{O}$ can be realized and the optimal trajectory is generated by the following sequence of unitary operations:

$$\mathbb{1}=U(0)\to U_{\mathrm{DF}}(t)\to U(t_f)=\mathcal{O}. \tag{44}$$

Thus, for sufficiently fast switching ability, we obtain optimal solutions which are: (i) independent of the spectral function, (ii) independent of the number of uncorrelated baths, (iii) independent of bath temperature, and (iv) all four gate quantifiers take the ideal values.[53] Because the Hamiltonian is time dependent, the problem of finding the optimal solution is best solved numerically.

2. Ideal model with full control

In this subsection we present numerical results within the strategy presented before. In all examples we study two coupled qubits and the CNOT-gate[54] operation as the target operator $\mathcal{O}$. Minimization was performed using standard line-search methods from the MATLAB optimization toolbox.

Our first quantum gate example demonstrates how one can find numerical solutions for optimal control fields if one has independent control over the single qubits and the qubit-qubit interaction. Furthermore, we first assume that there are no restrictions in the field strengths. To implement the optimal trajectory (44), it is convenient to split the control Hamiltonian into two parts:

$$H(t)=H_{\mathrm{DF}}+H_c(t), \tag{45}$$

where H_{DF} is given by Eq. (41) with time-independent

$$\hbar\omega_0=\varepsilon_{\mathrm{stat}}=\hbar\frac{n\pi}{t_f}, \tag{46}$$

where the integer $n=0,1,2,3\ldots$ ensures $U_{\mathrm{DF}}(t_f)=\mathbb{1}$. We use $n=0$ as a reference solution to check the improvement of the cost functional for increasing n. The second part $H_c(t)$ is optimized. To find $H_c(t)$ it is sufficient to consider the unitary problem and to minimize the cost functional (10) because H_{DF} ensures suppression of dissipation when n is increasing. We write

$$H_c(t)=H_1(t)+H_2(t)+H_{qq}(t) \tag{47}$$

with $H_1(t)=[\varepsilon_z^1(t)\sigma_z+\varepsilon_x^1(t)\sigma_x]\otimes\mathbb{1}$ and $H_2(t)=\mathbb{1}\otimes[\varepsilon_z^2(t)\sigma_z+\varepsilon_x^2(t)\sigma_x]$. In our example the qubit-qubit interaction is of the Heisenberg form

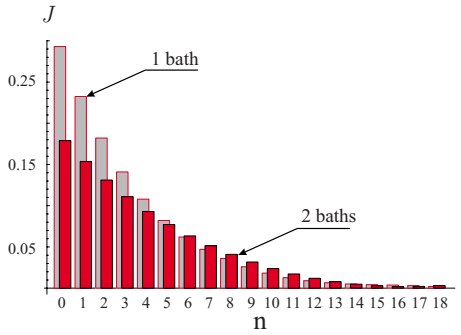

FIG. 3. (Color online) The plot shows the convergence of the cost functional $\mathcal{J}$ [Eq. (9)] when n, a measure of the static field (46), is increased. The cases of one bath and two baths are considered.

$$H_{qq}(t)=f(t)\sum_{k=1}^{3}\sigma_k\otimes\sigma_k, \tag{48}$$

where the qubit-qubit interaction $f(t)$ is controllable independently from the single-qubit control fields $\varepsilon_i^j(t)$. Without loss of generality we set $\varepsilon_z^1=$const. In total there are four independent control fields. Each field is expressed as

$$\varepsilon(t)=\frac{\hbar}{t_f}\sum_{j=1}^{F}a_j\sin\left(j\pi\frac{t}{t_f}\right), \tag{49}$$

and, for $F=6,24$ coefficients are free for variation.[55] The corresponding time-evolution operator factorizes into $U(t)=U_{\mathrm{DF}}(t)U_c(t)$. The equation of motion for $U_c(t)$ is simply $i\hbar\dot{U}_c(t)=U_{\mathrm{DF}}^{+}(t)H_c(t)U_{\mathrm{DF}}(t)U_c(t)$; $U_c(0)=\mathbb{1}$ and $U_c(t_f)=\mathcal{O}$. We minimize the cost functional (10) numerically to determine the coefficients a_j. The convergence of the procedure is shown in Fig. 3, where we collect data obtained by evaluating the cost functional (9) for the dissipative system. For completeness we consider both cases: one common and two distinct baths. We remark that all computed fields (two sets are shown in Fig. 4) are "good" unitary solutions. The cost functional (10) in any case is in the range $\mathcal{J}_u\approx 10^{-3}-10^{-4}$ which is quite sufficient compared to the change in $\mathcal{J}$ under the action of the dissipator. Obviously one can replace the static field $\varepsilon_{\mathrm{stat}}$ by an appropriate time-dependent field to fulfill boundary conditions of the control; for example, $\varepsilon_x^{1,2}(0)=\varepsilon_x^{1,2}(t_f)=0$. To obtain the results in Fig. 3 we used the parameters $\omega_c t_f=10$, $\eta=10^{-3}$, and $\beta\hbar\omega_c=20$. For $t_f=0.5$ ns we have a temperature of $T\approx 7.6$ mK and a decay rate, given by Eq. (B3), $\Gamma_\infty=62.8\times 10^6$ s^{-1}. This corresponds to a dephasing time $T_2\approx 1/\Gamma_\infty$ of the order of 10 ns. Measured Ramsey dephasing times for coupled SQUIDs are of the order[14] of 200 ns. We note that the cost functional $\mathcal{J}$ is proportional to η^2 for $\mathcal{J}_u\equiv 0$ as follows from perturbation theory (see Appendix B).

C. Limited control

In experiments there are several restrictions. The most important one is the limited control over the Hamiltonian. Two further restrictions lie in the maximal field strength

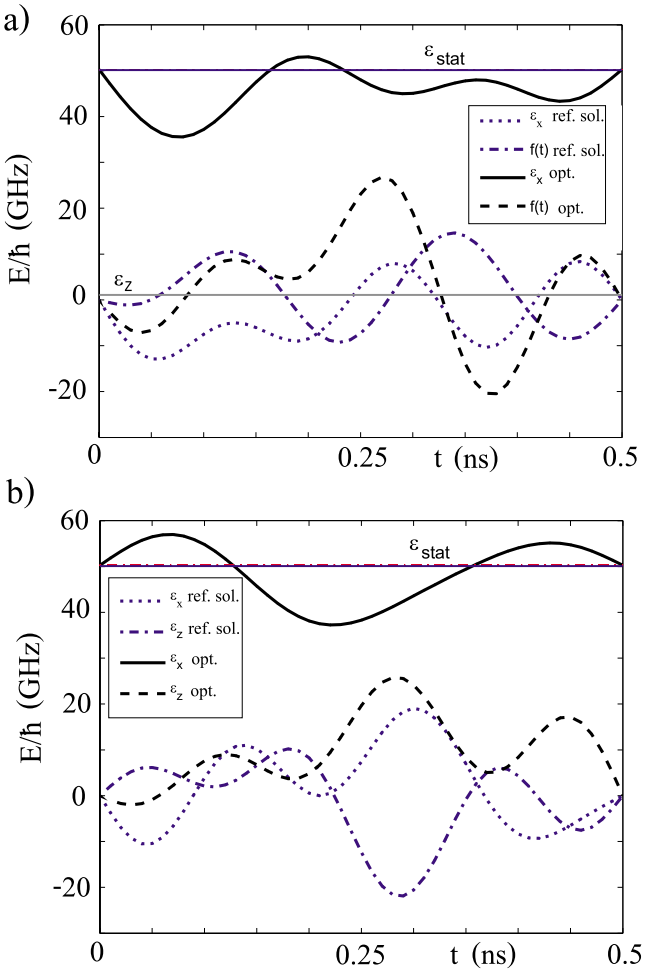

FIG. 4. (Color online) Control fields for both qubits. (a) Qubit 1 and qubit-qubit interaction. (b) Qubit 2 for $n=8$ and 0 for a target time $t_f=0.5$ ns corresponding to the static field (energy) $\varepsilon_{\text{stat}} \approx 32\ \mu\text{eV}$.

which can be realized and the fastest gate operation time. In general, these constraints hinder a direct realization of the optimal trajectory (44). To give a concrete example we consider a register of two charge qubits with tunable qubit-qubit interaction as discussed by Makhlin *et al.*[13] The control Hamiltonian for both qubits is given by

$$H(t) = \frac{1}{2}[\varepsilon_x^1(t)\sigma_x \otimes \mathbb{1} + \varepsilon_z^1(t)\sigma_z \otimes \mathbb{1}] + \frac{1}{2}[\varepsilon_x^2(t)\mathbb{1} \otimes \sigma_x + \varepsilon_z^2(t)\mathbb{1} \otimes \sigma_z] + H_{qq}(t), \quad (50)$$

where the qubit-qubit interaction has the form[36]

$$H_{qq}(t) = -K\varepsilon_x^1(t)\varepsilon_x^2(t)\sigma_y \otimes \sigma_y \quad (51)$$

with K as a parameter fixed by the inductivity of the inductor of the register of the coupled qubits. In our numerical computation it is equal $2t_f/\hbar$. The $\varepsilon_x^{1,2}(t)$ control of each qubit is realized by external magnetic fields, whereas $\varepsilon_z^{1,2}(t)$ is controlled using gate voltages. Even though this qubit-qubit interaction allows a realization of the CNOT gate with negligible error in isolated systems, the situation changes when dissipation is present and we cannot expect to reach values of $\mathcal{J}$ as low as before. All control fields are expressed as in Eq. (49) with $F=10$ variable coefficients. The qubit-qubit interaction (51) inhibits reaching the decoherence-free superoperator with the control Hamiltonian (41). We chose therefore another cost functional with a weight factor α where the prescription of the trajectory is weakened[56]

$$\mathcal{J}_{lc} = \mathcal{J}_u + \alpha \int_0^{t_f} dt' \left\{ N - \frac{1}{N} |\text{Tr}[U(t')U_{\text{DF}}^\dagger(t')]|^2 \right\}. \quad (52)$$

We set $\alpha=0.001$ in our numerical computations. Again $U_{\text{DF}}(t)$ is the decoherence-free time-evolution operator depending on n through Eq. (46). All parameters characterizing the environment are chosen as in the previous example. Table I shows results obtained by minimization of $\mathcal{J}_{lc}$ and subsequent evaluation of Eq. (9). We checked also the optimal solution by further optimization of the full cost functional (9). Its value remains essentially the same which confirms the independence of the solution from the details of the reservoir properties. We have, in any case, $\mathcal{J}_u \approx 10^{-4}-10^{-7}$. In Table I we employ the solution with $\alpha=0$ as a reference, which provides a minimum for Eq. (10) without the dissipator. Even if we cannot realize the trajectory (44) exactly, the results are comparable with the ones in Fig. 3, but we cannot expect a convergence behavior $\mathcal{J}\to 0$ for $n\to\infty$ as before.

TABLE I. Realization of the CNOT gate with limited control cost functional (9).

$n/\varepsilon_{\text{stat}}[\mu\text{eV}]$	5/20	10/40	Ref. sol. ($\alpha=0$)
$\mathcal{J}$ (two baths)	0.117	0.010	0.150
$\mathcal{J}$ (one bath)	0.182	0.017	0.216

Finally in Fig. 5 we summarize typical numerical results. Reference solution and optimal control fields are plotted in (a) and (b) for both qubits, respectively. In (c) we show the dependence of the cost functional on bath temperature. As one expects the quality of the solution decreases with increasing temperature. In part (d) we present the time evolution of the diagonal elements of the density matrix for a specific input state under the optimal control fields. Rapid oscillations are the consequence of the high-field strengths and document the strategy of Eq. (39).

D. Conclusions and relevance to experiment

Various other qubit-qubit coupling models have been discussed in the literature such as[13,31]

$$H_{qq}(t) = f(t)\sigma_z \otimes \sigma_z, \quad (53)$$

$$H_{qq}(t) = f(t)(\sigma^+ \otimes \sigma^- + \sigma^- \otimes \sigma^+). \quad (54)$$

Here we use $\sigma^\pm = (\sigma_x \pm i\sigma_y)/2$. As long as dissipation is weak, the presented strategy for controlling quantum gates is applicable. Moreover, if the experimental situation is such that the dissipationless system allows generation of the target operation, then one can find optimal solutions in the pro-

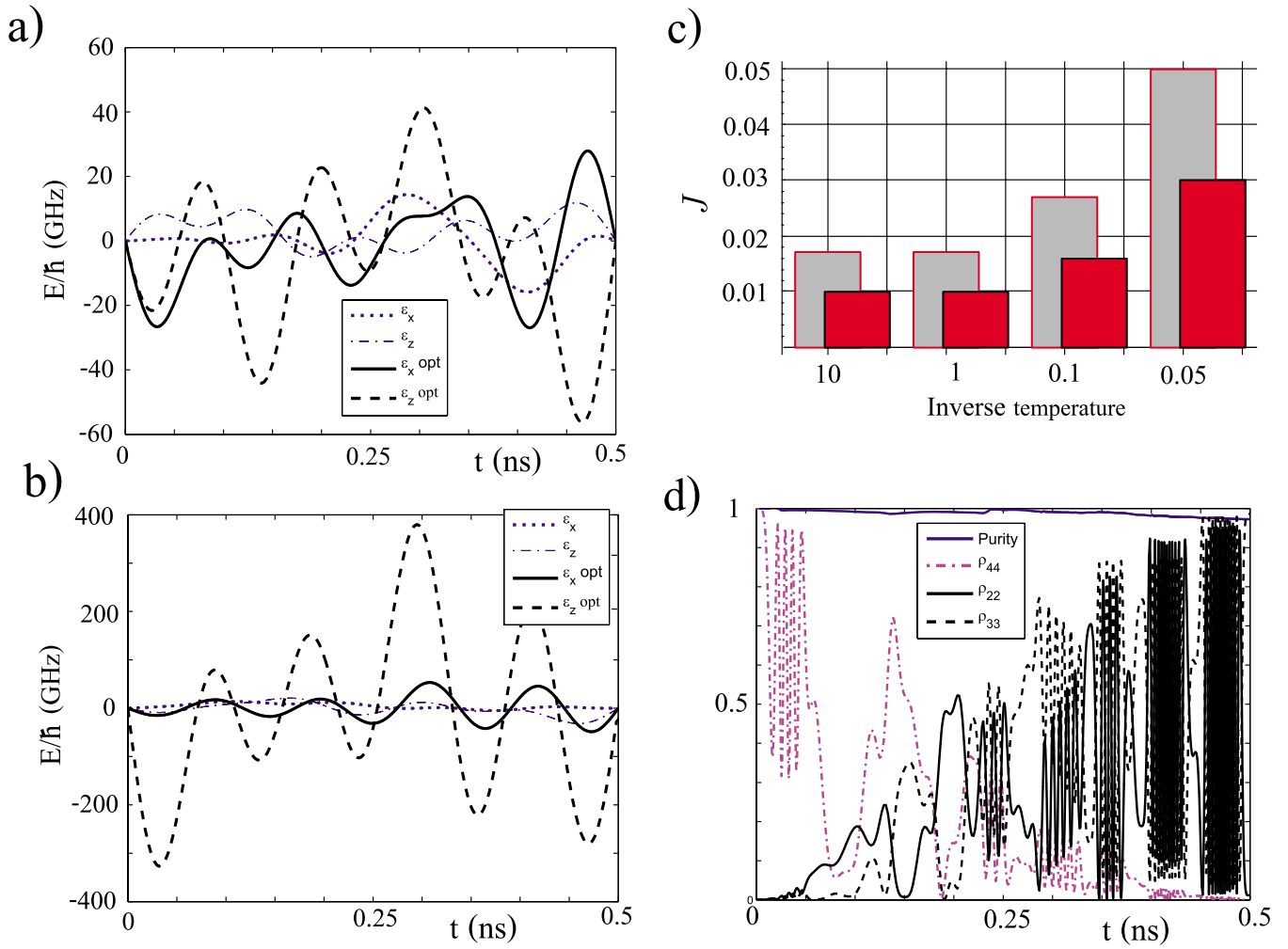

FIG. 5. (Color online) (a) and (b) Control fields for the qubits for the CNOT gate for $n=10$, the optimal solution, and the unitary solution $\alpha=0$ in Eq. (52). (c) shows the cost functional $\mathcal{J}$ for different inverse temperatures β, where $\beta=1$ corresponds to $T=7.6$ mK. Gray (light gray) bars for one bath and red (dark gray) bars for two baths. In (d) we show the time evolution of the initial state $\rho(0)=|4\rangle\langle 4|$ under the optimal Hamiltonian with $n=10$. The rapid oscillations demonstrate clearly the optimization strategy (39). The purity $\mathrm{Tr}[\rho(t)^2]$ remains nearly constant.

posed fashion. Furthermore, if the qubit-qubit coupling is of Heisenberg type with a control field, which is determined (up to a constant factor) by the four single-qubit control fields only, one's ability to combat dephasing is severely limited. Hence design of multiqubit systems that do not suffer from this restriction is desirable.

If one describes the relaxation by fixed rates, for example within a Lindblad equation, one loses the control-field dependence of the effective subsystem-environment interaction expressed in Eq. (39) and, as a consequence, loses the convergence property (43). This demonstrates the importance of a microscopic modeling of the system bath interaction for the theorist. For the experimentalist it implies the need for control fields which are applicable at a sufficiently short-time scale and strength such that the effective quantum subsystem-bath interaction can be manipulated. Furthermore, this analysis has shown that, for "reasonable" quantum gate realizations with weak dissipative effects, there exist optimal solutions for which one can focus on the implementation of the target unitary operation since they almost automatically minimize dissipation. In other words, there exists a subset to the solutions for the dissipation-free system which, in nearly unmodified form, minimizes dissipative effects.

VI. SUMMARY

In this paper we present a general optimal control theory for quantum subsystems based on the superoperator formalism. It has an advantage over previous work; that is, it does not require sampling over possible initial states. Thus it avoids all the problems associated with proper selection of this ensemble regarding relevance, orthogonality, and completeness. Applied to weakly dissipative systems, it reduces to an earlier approach developed by us. Applied to unitary time evolution, it reduces to standard formulations.

This approach was used to study quantum gates within a spin-boson model for dephasing and a Heisenberg-type qubit-qubit interaction. The dissipator was computed within second-order perturbation theory in the spin-boson interaction leading to a control-field dependence in the effective

subsystem-bath interaction, which we show to be essential for an efficient suppression of dissipative effects. Focusing on solid-state-based double-qubit systems, in particular SQUID-based implementations, we are able to identify a decoherence-free subspace for the superoperator. In an ideal situation where each of the two-qubit control fields and the qubit-qubit interaction can be controlled independently and the control-field shapes are unlimited, one is able to make decoherence (dephasing) arbitrarily small for arbitrary gate operation. We demonstrate this numerically for the CNOT gate.

For such an ideal model we presented optimal solutions which are independent of the spectral function, independent of the number of uncorrelated baths, independent of bath temperature, and for which all four gate quantifiers take the prescribed ideal values. In the realistic situation of current SQUID-based qubit designs, where the qubit-qubit coupling cannot be controlled independently from the single-qubit control fields, one's control of dephasing effects is clearly reduced; however, we are able to present a family of exact solutions for the unitary problem that lies very close to optimal solutions for the dissipative quantum gate. Using realistic control field characteristics from experiment, we arrive at optimized gate operations which deviate from the desired operation by a few percent in the cost functional, depending on bath temperature, corresponding to a predicted gate fidelity of clearly better than 90%.

ACKNOWLEDGMENTS

M.W. thanks U. Hohenester for discussion. We wish to acknowledge financial support of this work by FWF Austria under Project No. P18829.

APPENDIX A: PERTURBATION THEORY FOR THE EVOLUTION SUPEROPERATOR

In this appendix we outline the derivation of first-order perturbation theory for the time-evolution superoperator and a general dissipation superoperator $\mathcal{D}_{ijmn}(t)$. We start with Eq. (31). The zeroth-order superoperator $\mathcal{X}^{(0)}_{ijrs}(t) = U_{ir}(t)U^{\dagger}_{sj}(t)$ is an exact solution of Eq. (31) without dissipator. We set $\mathcal{X}^{(1)}_{ijrs}(t) = \mathcal{X}^{(0)}_{ijrs}(t) + \delta\mathcal{X}_{ijrs}(t)$ and obtain for the deviation $\delta\mathcal{X}_{ijrs}(t)$ the equation

$$\delta\dot{\mathcal{X}}_{ijrs}(t) = -\frac{i}{\hbar}\mathcal{L}_{ijmn}(t)\delta\mathcal{X}_{mnrs}(t) - \mathcal{D}_{ijmn}(t)\mathcal{X}^{(0)}_{mnrs}(t). \tag{A1}$$

Here we have neglected the term $\mathcal{D}_{ijmn}(t)\delta\mathcal{X}_{mnrs}(t)$ because it is quadratically in the dissipator (the coupling strength η). To solve this system of differential equations we make the ansatz

$$\delta\mathcal{X}_{ijrs}(t) = \mathcal{X}^{(0)}_{ijmn}(t)\delta\tilde{\mathcal{X}}_{mnrs}(t). \tag{A2}$$

We eliminate the term containing $\mathcal{L}_{ijmn}(t)$ and remain with the equation

$$\mathcal{X}^{(0)}_{ijmn}(t)\delta\dot{\tilde{\mathcal{X}}}_{mnrs}(t) = -\mathcal{D}_{ijmn}(t)\mathcal{X}^{(0)}_{mnrs}(t). \tag{A3}$$

Furthermore, using the orthonormality

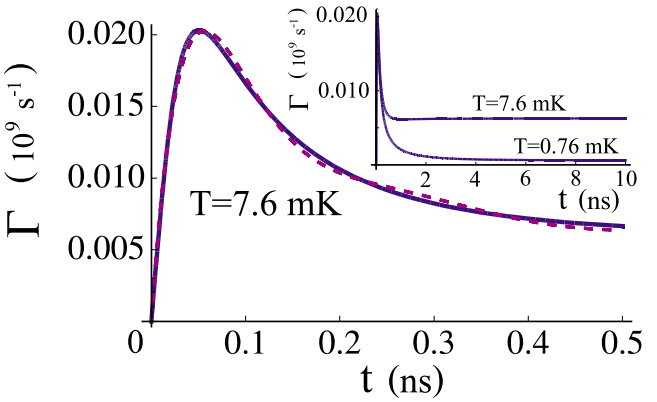

FIG. 6. (Color online) Decay rate $\Gamma(t)$ defined by Eq. (B1). The blue (dark gray) solid line is the exact function and the cyan (light gray) dotted line corresponds to the approximation. The inset shows the rates for two different temperatures at longer (Markovian) time scales (thermal regime). Parameters: $\hbar\beta\omega_c = 20$ and $\eta = 10^{-3}$.

$$\mathcal{X}^{(0)}_{ijmn}(t)\mathcal{X}^{(0)}_{jilk}(t) = \delta_{km}\delta_{nl} \tag{A4}$$

we can isolate $\delta\dot{\tilde{\chi}}(t)$. After integration and insertion into Eq. (A2) we obtain

$$\delta\mathcal{X}_{ijrs}(t) = -\mathcal{X}^{(0)}_{ijmn}(t)\int_0^t dt'\mathcal{D}_{klpq}(t')\chi^{(0)}_{pqrs}(t')\mathcal{X}^{(0)}_{lkmn}(t'). \tag{A5}$$

This result is quite general. It is valid for a time-dependent relaxation tensor as well as for a dissipator described by fixed rates. From this expression one obtains, using the Cauchy-Schwarz inequality,

$$\begin{aligned}\|\delta\chi\|^2 &\equiv \sum_{i,j,r,s} |\delta\chi_{ijrs}(t_f)|^2 \\ &\le t_f \sum_{i,j,r,s}\int_0^{t_f} |\mathcal{D}_{ijrs}(t')|^2 dt' \\ &\equiv t_f \int_0^{t_f} \|\mathcal{D}(t')\|^2 dt'.\end{aligned} \tag{A6}$$

For $\mathcal{X}^{(0)}(t_f) = \mathcal{X}_T$, this inequality gives

$$\mathcal{J} \le t_f \int_0^{t_f} \|\mathcal{D}(t')\|^2 dt'. \tag{A7}$$

Given the dissipator superoperator this relation gives an upper limit for dissipative effects to the superoperator cost functional and, hence, a measure for the maximum fidelity loss due to dissipation that any unitary solution for the ideal quantum system can suffer. We also remark that this result does not depend on the target operator $\mathcal{X}_T$.

APPENDIX B: DECOHERENCE FUNCTION

The intrinsic properties of decoherence of an open quantum system are expressed in terms of the decoherence function. We define the decoherence function by

$$\Gamma(t) := \int_0^t [C(t-t') + C^*(t-t')]dt', \tag{B1}$$

where $C(t-t')$, in turn, is defined in Eq. (20). Using these definitions, one obtains, for a subsystem with $H(t)=0$, the decay rates for the off-diagonal elements of its density matrix $\rho(t)$. For example, one obtains the equations $\dot{\rho}_{12}(t) = -2\Gamma(t)\rho_{12}(t)$ for the two-level system, $\dot{\rho}_{14}(t) = -4\Gamma(t)\rho_{14}(t)$ for two qubits coupled to two identical uncorrelated baths, and $\dot{\rho}_{14}(t) = -8\Gamma(t)\rho_{14}(t)$ if two qubits are coupled to one common bath. Figure 6 shows the decoherence function and its form when eight Laguerre polynomials are used to approximate $C(t-t')$. Evaluation of the integral (B1) for an Ohmic spectrum [Eq. (21)] gives a decoherence function

$$\Gamma(t) = -\frac{2\eta\omega_c^2 t}{1+(\omega_c t)^2} + \frac{4\eta}{\hbar\beta}\mathrm{Im}\left[\psi\left(\frac{1+i\omega_c t}{\beta\hbar\omega_c}\right)\right]. \tag{B2}$$

In the Markovian limit $\omega_c t \to \infty$, we obtain a time-independent rate (see the inset of Fig. 6)

$$\Gamma_\infty = \frac{2\eta\pi}{\hbar\beta}. \tag{B3}$$

*markus.wenin@uni-graz.at
†walter.poetz@uni-graz.at

[1] H. J. Krenner, S. Stufler, M. Sabathil, E. Clark, P. Ester, M. Bichler, G. Abstreiter, J. Finley, and A. Zrenner, New J. Phys. **7**, 184 (2005).
[2] G. Burkard, D. Loss, and D. P. DiVincenzo, Phys. Rev. B **59**, 2070 (1999).
[3] B. W. Lovett, J. H. Reina, A. Nazir, and G. A. Briggs, Phys. Rev. B **68**, 205319 (2003).
[4] T. Calarco, A. Datta, P. Fedichev, E. Pazy, and P. Zoller, Phys. Rev. A **68**, 012310 (2003).
[5] E. Biolatti, I. D'Amico, P. Zanardi, and F. Rossi, Phys. Rev. B **65**, 075306 (2002).
[6] Y. Wu, X. Li, L. M. Duan, D. G. Steel, and D. Gammon, Phys. Rev. Lett. **96**, 087402 (2006).
[7] C. Emary and L. J. Sham, Phys. Rev. B **75**, 125317 (2007).
[8] U. Hohenester and G. Stadler, Phys. Rev. Lett. **92**, 196801 (2004).
[9] U. Hohenester, Phys. Rev. B **74**, 161307(R) (2006).
[10] S. Vorojtsov, E. R. Mucciolo, and H. U. Baranger, Phys. Rev. B **71**, 205322 (2005).
[11] M. Thorwart, J. Eckel, and E. R. Mucciolo, Phys. Rev. B **72**, 235320 (2005).
[12] M. J. Storcz, U. Hartmann, S. Kohler, and F. K. Wilhelm, Phys. Rev. B **72**, 235321 (2005).
[13] Y. Makhlin, G. Schön, and A. Shnirman, Rev. Mod. Phys. **73**, 357 (2001).
[14] A. O. Niskanen, K. Harrabi, F. Yoshihara, S. Lloyd, and J. S. Tsai, Science **316**, 723 (2007).
[15] T. Yamamoto, M. Watanabe, J. Q. You, Y. A. Pashkin, O. Astafiev, Y. Nakamura, F. Nori, and J. S. Tsai, Phys. Rev. B **77**, 064505 (2008).
[16] T. Yamamoto, Y. A. Pashkin, O. Astafiev, Y. Nakamura, and J. S. Tsai, Nature (London) **425**, 941 (2003).
[17] M. J. Storcz and F. K. Wilhelm, Phys. Rev. A **67**, 042319 (2003).
[18] M. Governale, M. Grifoni, and G. Schön, Chem. Phys. **268**, 273 (2001).
[19] R. Roloff, M. Wenin, and W. Pötz, Proceedings of the IWCE–12, 2007 (unpublished).
[20] A. E. Bryson and Y. C. Ho, *Applied Optimal Control* (Hemisphere, New York, 1975).
[21] Y. Ohtsuki, G. Turinici, and H. Rabitz, J. Chem. Phys. **120**, 5509 (2004).
[22] S. E. Sklarz, D. J. Tannor, and N. Khaneja, Phys. Rev. A **69**, 053408 (2004).
[23] M. Branderhorst, P. Londero, P. Wasylczyk, C. Brif, R. Kosut, H. Rabitz, and I. Walmsley, Science **320**, 638 (2008).
[24] R. Roloff and W. Pötz, Phys. Rev. B **76**, 075333 (2007).
[25] H. Jirari and W. Pötz, Phys. Rev. A **72**, 013409 (2005).
[26] M. Wenin and W. Pötz, Appl. Phys. Lett. **92**, 103509 (2008).
[27] S. Pasini, T. Fischer, P. Karbach, and G. S. Uhrig, Phys. Rev. A **77**, 032315 (2008).
[28] M. Grace, C. Brif, H. Rabitz, I. A. Walmsley, R. L. Kosut, and D. A. Lidar, J. Phys. B **40**, S103 (2007).
[29] A. Spörl, T. Schulte-Herbrüggen, S. J. Glaser, V. Bergholm, M. J. Storcz, J. Ferber, and F. K. Wilhelm, Phys. Rev. A **75**, 012302 (2007).
[30] A. Spörl, T. Schulte-Herbrüggen, S. J. Glaser, V. Bergholm, M. J. Storcz, J. Ferber, and F. K. Wilhelm, Phys. Rev. A **75**, 012302 (2007).
[31] M. Thorwart and P. Hänggi, Phys. Rev. A **65**, 012309 (2001).
[32] M. S. Sarandy and D. A. Lidar, Phys. Rev. Lett. **95**, 250503 (2005).
[33] J. P. Palao and R. Kosloff, Phys. Rev. A **68**, 062308 (2003).
[34] H. Rabitz, M. Hsieh, and C. Rosenthal, Phys. Rev. A **72**, 052337 (2005).
[35] M. Hsieh and H. Rabitz, Phys. Rev. A **77**, 042306 (2008).
[36] A. O. Niskanen, J. J. Vartiainen, and M. M. Salomaa, Phys. Rev. Lett. **90**, 197901 (2003).
[37] R. Wu, A. Pechen, C. Brif, and H. Rabitz, J. Phys. A **40**, 5681 (2007).
[38] H. Breuer and F. Petruccione, *The Theory of Open Quantum Systems* (Oxford University Press, Oxford, 2002).
[39] M. Wenin and W. Pötz, Phys. Rev. A **78**, 012358 (2008).
[40] A. Leggett, S. Chakravarty, A. T. Dorsey, M. P. A. Fisher, A. Garg, and W. Zwerger, Rev. Mod. Phys. **59**, 1 (1987).
[41] K. Blum, *Density Matrix Theory and Applications*, 2nd ed. (Plenum, New York, 1996).
[42] D. P. DiVincenzo and D. Loss, Phys. Rev. B **71**, 035318 (2005).
[43] H. Jirari and W. Pötz, Phys. Rev. A **74**, 022306 (2006).
[44] W. Pötz, Appl. Phys. Lett. **89**, 254102 (2006).
[45] C. Hilbert, *Methoden der Mathematischen Physik* (Springer-Verlag, Berlin, 1993).
[46] M. Wenin and W. Pötz, Phys. Rev. A **74**, 022319 (2006).
[47] R. Fazio, G. M. Palma, and J. Siewert, Phys. Rev. Lett. **83**, 5385

(1999).
[48] R. Roloff and W. Pötz (unpublished).
[49] O. Astafiev, Y. A. Pashkin, Y. Nakamura, T. Yamamoto, and J. S. Tsai, Phys. Rev. Lett. **93**, 267007 (2004).
[50] D. A. Lidar, I. L. Chuang, and K. B. Whaley, Phys. Rev. Lett. **81**, 2594 (1998).
[51] L. Viola, E. Knill, and S. Lloyd, Phys. Rev. Lett. **82**, 2417 (1999).
[52] R. I. Karasik, K. P. Marzlin, B. C. Sanders, and K. B. Whaley, Phys. Rev. A **77**, 052301 (2008).
[53] J. Poyatos, J. Cirac, and P. Zoller, Phys. Rev. Lett. **78**, 390 (1997).
[54] M. A. Nielsen and I. L. Chuang, *Quantum Computation and Quantum Information* (Cambridge University Press, Cambridge, 2004).
[55] This ansatz is chosen such that the field vanishes at the endpoints of the interval $[0,t_f]$.
[56] The system of kinetic equations in this case consists of the usual von Neumann equation for $U(t)$ and an auxiliary equation $\dot{\mathcal{J}}_{dfs}(t)=\alpha[N-\frac{1}{N}|\mathrm{Tr}\{U(t)U_{\mathrm{DF}}^{+}(t)\}|^2]$. All differential equations are solved in parallel.